Supplemental Material for : Modeling serological testing to inform relaxation of social distancing for COVID-19 control

Alicia N. M. Kraay[1,a], Kristin N. Nelson[1,a], Conan Zhao[2,3], David Demory[2], Joshua S. Weitz[2,4,b], Benjamin A. Lopman[1,b]

[1] Rollins School of Public Health, Emory University, Atlanta, GA, USA
[2] School of Biological Sciences, Georgia Institute of Technology, Atlanta, GA, USA
[3] Interdisciplinary Graduate Program in Quantitative Biosciences, Georgia Institute of Technology, Atlanta, GA, USA
[4] School of Physics, Georgia Institute of Technology, Atlanta, GA, USA

November 13, 2020

S1. Model Equations

The ordinary differential equations describing the model are shown below for group i. The positive test group is denoted with the '+' sign.

[a]These authors contributed equally to this work
[b]These authors contributed equally to this work

$$
\begin{aligned}
\frac{dS_i}{dt} &= -\lambda_i(t)S_i - (1-sp)\times test_i(t)S_i \\
\frac{dE_i}{dt} &= \lambda_i(t)S_i - \gamma_e E_i - (1-sp)\times test_i(t)E_i \\
\frac{dI_{s,i}}{dt} &= \gamma_e E_i p - \gamma_s I_{s,i} \\
\frac{dI_{a,i}}{dt} &= \gamma_e E_i(1-p) - \gamma_a I_{a,i} - (1-sp)\times test_i(t)I_{a,i} \\
\frac{dH_{s,i}}{dt} &= \gamma_s I_{s,i}(Hosp_i - Crit_i) + \gamma_s I^+_{s,i}(Hosp_i - Crit_i) - \gamma_{hs}H_{s,i} \\
\frac{dH_{c,i}}{dt} &= \gamma_s I_{s,i} Crit_i + \gamma_s I^+_{s,i} Crit_i - \gamma_{hc}H_{c,i} \\
\frac{dD_i}{dt} &= \gamma_{hc}H_{c,i}Die_i \\
\frac{dR_i}{dt} &= (1-Hosp_i)\gamma_s I_{s,i} + \gamma_a I_{a,i} + (1-se)\times m_2(t)\gamma_{hs}H_{s,i} + (1-se)\times m_2(t)\gamma_{hc}H_{c,i}(1-Die_i) \\
&\quad - se\times test_i(t)R_i + m_1(t)\gamma_{hs}H_{s,i} + m_1(t)\gamma_{hc}H_{c,i}(1-Die_i) \\
\frac{dS^+_i}{dt} &= (1-sp)test_i(t)S_i - \lambda^+_i(t)S^+_i \\
\frac{dE^+_i}{dt} &= (1-sp)test_i(t)E_i + \lambda^+_i(t)S^+_i - \gamma_e E^+_i \\
\frac{dI^+_{s,i}}{dt} &= \gamma_e E^+_i p - \gamma_s I^+_{s,i} \\
\frac{dI^+_{a,i}}{dt} &= (1-sp)\times test_i(t)I_{a,i} + \gamma_e E^+_i(1-p) - \gamma_a I^+_{a,i} \\
\frac{dR^+_i}{dt} &= se\times test_i(t)R_i + se\gamma_{hc}m_2(t)H^+_{c,i}(1-Die_i) + \\
&\quad se\times m_2(t)\gamma_{hs}H_{s,i} + (1-Hosp_i)\gamma_s I^+_{s,i} + \gamma_a I^+_{a,i}
\end{aligned}
$$

$m_1(t)$ and $m_2(t)$ are defined as follows (t_{start} is when testing starts, on November 1, 2020):

$$
m_1(t) = \begin{cases} 1 & t < t_{start} \\ 0 & t \geq t_{start} \end{cases}
$$

$$
m_2(t) = \begin{cases} 0 & t < t_{start} \\ 1 & t \geq t_{start} \end{cases}
$$

The force of infection $\lambda(t)$ for the i-th group is a function of the number of social contacts for age group i with each subgroup j at time t ($x_{i,j}(t)$), the probability of infection given contact (q), the number of infections in each group at time t ($infec_j(t)$), and the population size of each group at time t ($n_j(t)$). The overall equation for $\lambda_i(t)$ is shown below:

$$\lambda_i(t) = q\Bigg[\frac{x_{i,ch}(t)infect_{ch}(t)}{n_{ch}(t)} + \frac{x_{i,ch^+}(t)infect_{ch^+}(t)}{n_{ch^+}(t)} + \frac{x_{i,ad}(t)infect_{ad}(t)}{n_{ad}(t)}) + \frac{x_{i,ad^+}(t)infect_{ad^+}(t)}{n_{ad^+}(t)} + \frac{x_{i,rc}(t)infect_{rc}(t)}{n_{rc}(t)} + \frac{x_{i,rc^+}(t)infect_{rc^+}(t)}{n_{rc^+}(t)} + \frac{x_{i,fc}(t)infect_{fc}(t)}{n_{fc}(t)}) + \frac{x_{i,fc^+}(t)infect_{fc^+}(t)}{n_{fc^+}(t)} + \frac{x_{i,el}(t)infect_{el}(t)}{n_{el}(t)}) + \frac{x_{i,el^+}(t)infect_{el^+}(t)}{n_{el^+}(t)}\Bigg]$$

i and j take values of ch (children age 0-19 years), ad (adults age 20-65 years who are not working or working from home), el (older adults 65+ years of age), rc (adults at work in 'reduced-contact' occupations, where they have fewer contacts than pre-pandemic), fc (adults as work in full contact occupations, where they have the same number of contacts as pre-pandemic).

The number of infectious individuals by age group and test status is equal to the sum of documented (symptomatic) cases and a fraction of the undocumented (asymptomatic) cases, where this fraction asy corresponds to the relative infectiousness of undocumented cases. This is shown below for children:

$$infect_{ch}(t) = asyI_{a,ch} + I_{s,ch}$$

S2. Model parameters

We defined the three metropolitan areas in the same way as Havers et al [1]. For Washington Puget Sound metropolitan region, we included death data from King, Snohomish, Pierce, Kitsap and Grays Harbor counties. For the New York City metropolitan region, we included data from Manhattan, Bronx, Queens, Kings, and Nassau Counties. For the South Florida metropolitan region, we included data from Miami-Dade, Broward, Palm Beach, and Martin counties. These same counties were also used to derive age-specific population sizes for each region.

Parameters used in the model simulations are shown in Table S1. We assume that the size of the working population is stable over the duration of the simulation. Although this may not be the case as unemployment increases throughout the pandemic, the rate at which unemployment has changed so far has been time-varying and its future trajectory is unknown.

Where possible, parameters were taken from prior literature. However, data from the initial stages of the outbreak were fitted for the probability of infection per contact (q), the fraction of infections symptomatic (p), the initial intensity of social distancing for workplace contacts ($p_{reduced}$) and for other contacts (sd_{other}). These parameters were fitted to initial outbreak dynamics from each of the three metropolitan locations. While q does not vary with time, we acknowledge that some control measures such as masking may result in changes in the probability of infection given contact over the course of the pandemic. In our model, changes in the contact matrix based on both the initial strength of social distancing ($p_{reduced}$ and sd_{other}) and its strength after reopening captures the contribution of both reducing the number of social contacts and changes in the likelihood of transmission from those contacts based on mask use and physical distancing.

We used the dates that stay-at-home orders were enacted, and later lifted, in each location and the dates corresponding to when local schools opened for at least partial in-person instruction in each location to inform dates of reopening in the model.

S3. Model fitting

Initial Conditions

We first calculate the number of weeks between the first death and the first week where the cumulative death toll exceeds 10. For example, in the South Florida region, the first death was reported the week of March 18, 2020. The two subsequent weeks saw the death toll rise to 6 and 42. Using region-specific conditions (population demographics, stay-at-home order and lift dates, and deaths data), we initialize an epidemic consisting of a single exposed adult ($a0$). We use baseline estimates for the parameters we aim to fit later (q = 0.0451, c = 1, $symptomatic\_fraction = 0.14$, $sd_{other} = 0.25$, $p_{reduced} = 0.1$). Note that $symptomatic\_fraction$ is equivalent to p in Table 2. We forward simulate a single-origin epidemic until the modeled number of deaths exceeds the number of deaths reported in the second week after the first death (in South Florida, 42 deaths), then use the distribution two weeks prior as our initial conditions. For MCMC fits, we additionally allow an error term, $init_{scale}$, such that the calculated distribution was scaled by $(1 + init_{scale})$ for each chain iteration. For fitting, we constrained q to $[0, 0.07]$ and $init_{scale}$ to $[0, \inf)$. All other parameters were constrained to $[0, 1]$.

Parameter	Code	Value	Units	Source(s)
Natural history				
Latent period	γ_e	1/3	1/days	[2]
Recovery rate, asymptomatic infections	γ_a	1/7	1/days	[3]
Recovery rate, symptomatic infections	γ_s	1/7	1/days	[3]
Recovery rate, hospitalized cases	γ_{hs}	1/5	1/days	[4]
Recovery rate, critical care cases	γ_{hc}	1/7	1/days	[4]
Relative infectiousness of asymptomatic infections	asy	0.55	–	[5, 6]
Hospitalization				
Probability of hospitalization				[7]
Children	$Hosp_{ch}$	0.061	–	
Adults	$Hosp_{ad}$	0.182	–	
Elderly	$Hosp_{el}$	0.417	–	
Probability of requiring critical care				[7]
Children	$Crit_{ch}$	0	–	
Adults	$Critc_{ad}$	0.063	–	
Elderly	$Crit_{el}$	0.173	–	
Probability of death among critical care patients				
Children	Die_{ch}	0	–	[8]
Adults	Die_{ad}	0.5	–	[5]
Elderly	Die_{el}	0.5	–	[5]
Test features				
Sensitivity	se	1.00	–	[9]
Specificity	sp	0.998 (0.5, 0.998)	–	[9]
Population features				
Population size				[10]
New York City		9.43e6	people	
South Florida		6.17e6	people	
Washington Puget Sound		4.06e6	people	
Baseline contact rates by age	$x_{i,j}$	see matrices		[11]
Adult working population segments, size				[12]
Exclusive work from home occupations	n_{home}	$0.316 \times n_{adult}$	people	
Reduced contact occupations	$n_{reduced}$	$0.628 \times n_{adult}$	people	
Full contact occupations	n_{full}	$0.057 \times n_{adult}$	people	
Fraction of adult population (20-65 years) in workforce		1.0		assumption
Intervention parameters				
Shielding	α	(0, 9)	per contact	varied
Fraction tested	$test_i(t)$	(0, 0.03)	proportion per day	varied

Table S1: Fixed parameters across locations used in model simulations. Values shown in parentheses represent a range, used to perform sensitivity analysis.

Parameter	Code	New York	South Florida	Washington	Units	Source(s)
Fitted parameters						
Fraction symptomatic[1]	p [2]	0.480	0.203	0.475	–	fitted
		(0.407, 0.555)	(0.185, 0.224)	(0.497, 0.519)		
Probability of infection per contact[3]	q	0.034	0.043	0.023	1/contact	fitted
		(0.032, 0.036)	(0.039, 0.045)	(0.022, 0.022)		
		(1.91, 2.12)	(2.57, 2.67)	(1.28, 1.31)		
Strength of social distancing maintained[1]	c	0.491	0.974	0.126	–	fitted
		(0.026, 0.965)	(0.923, 0.999)	(0.009, 0.337)		
Fraction of work contacts maintained (rc workers)[1]	$p.reduced$	0.323	0.367	0.800)	–	fitted
		(0.022, 0.678)	(0.016, 0.776)	(0.545, 0.979		
for rc occupations						
Fraction of 'other' contacts maintained[1]	$sd.other$ [5]	0.106	0.195	0.168	–	fitted
		(0.007, 0.555)	(0.014, 0.398)	(0.056, 0.294)		
Initial conditions scaling term[4]	–				–	fitted
		(0.005, 0.446)	(0.004, 0.490)	(0.0004, 0.042)		
Epidemic start date	t_0	Feb 20	Feb 27	Feb 13	date	fitted
Basic reproduction number	R_0	2.04	2.63	1.33	–	calculated from fitted value
Population features (fixed)						
Baseline contact rates by age	$x_{i,j}$		see matrices			[11]
US population age groups, size						[13, 10]
Children	n_{child}	2208909	1398572	974924	people	
Adults	n_{adult}	5944919	3679331	2563244	people	
Elderly	$n_{elderly}$	1283369	1090711	526665	people	
Intervention timing (fixed)						
Stay at home order start	–	Mar 16	Mar 17	Mar 16	date	[14, 15, 16]
Reopening	–	June 8	May 20	May 31	date	[14, 15, 16]
School reopening	–	Oct 1	Sept 1	Oct 1	date	assumption

[1] Constrained so fitted value would fall between 0 and 1

[2] Note that p is equivalent to $symptomatic\_fraction$ in Figures S1-S9

[3] Constrained so fitted value would fall between 0 and 0.07

[4] Constrained so fitted value would fall between 0 and infinity

[5] Note that $sd.other$ is equivalent to $socialDistancing\_other$ in Figures S1-S9

Table S2: Location-specific parameters used in model simulations. Values shown for fitted parameters are the maximum likelihood estimate, used for main text simulations in Figures 2 and 3, and values in parentheses represent the 95% CI, used to calculate simulation intervals

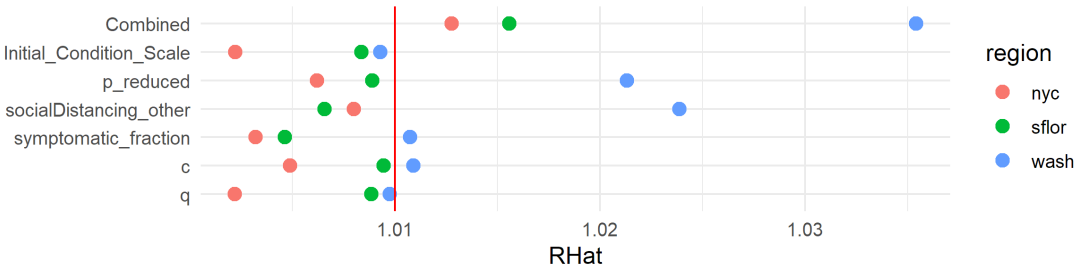

Figure S1: Gelman-Rubin diagnostics plot. We calculate Gelman-Rubin $\widehat{R}$ values for chain convergence among all 10 chains for New York City and South Florida. We excluded chain 3 for Washington because it did not converge. $\widehat{R}$ values for all parameters were below 1.1, with the majority under the 1.01 convergence threshold. [17]

MCMC

Using Markov Chain Monte Carlo (MCMC) we estimate the six model parameters listed in Table S2. We checked for chain convergence using the Gelman-Rubin diagnostic (Figure S1). Figures S2, S5, and S8 show the resulting trace plots, and Figures S3, S6, and S9 show the resulting joint distributions.

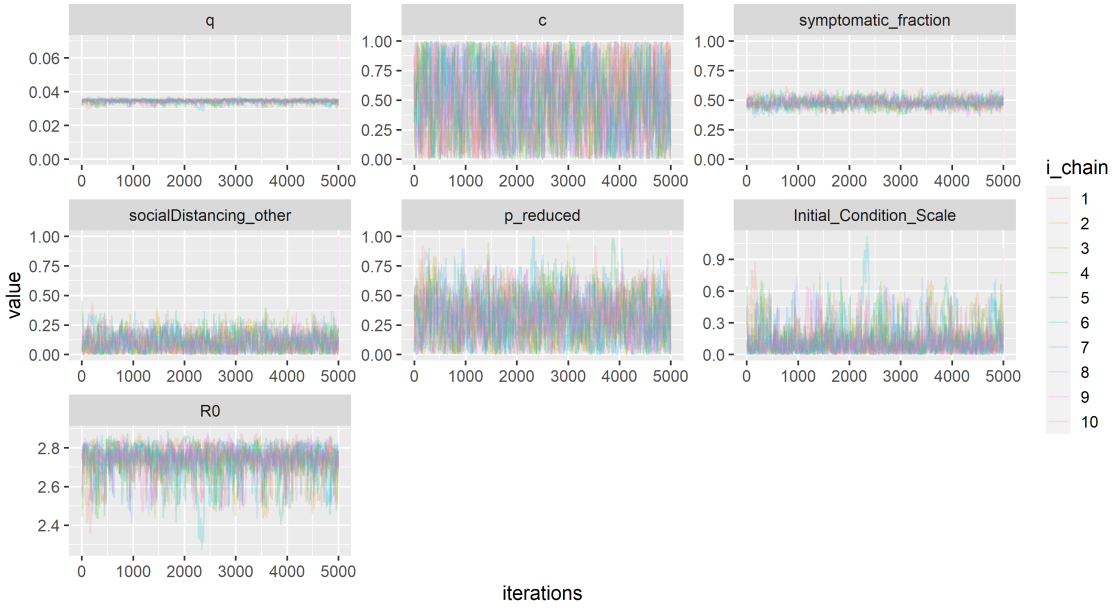

Figure S2: New York City Post-burn-in MCMC Traceplots. Y-axis ranges are limited to show parameter search space constraints. R_0 traces are calculated from q and $symptomatic\_fraction$ traces.

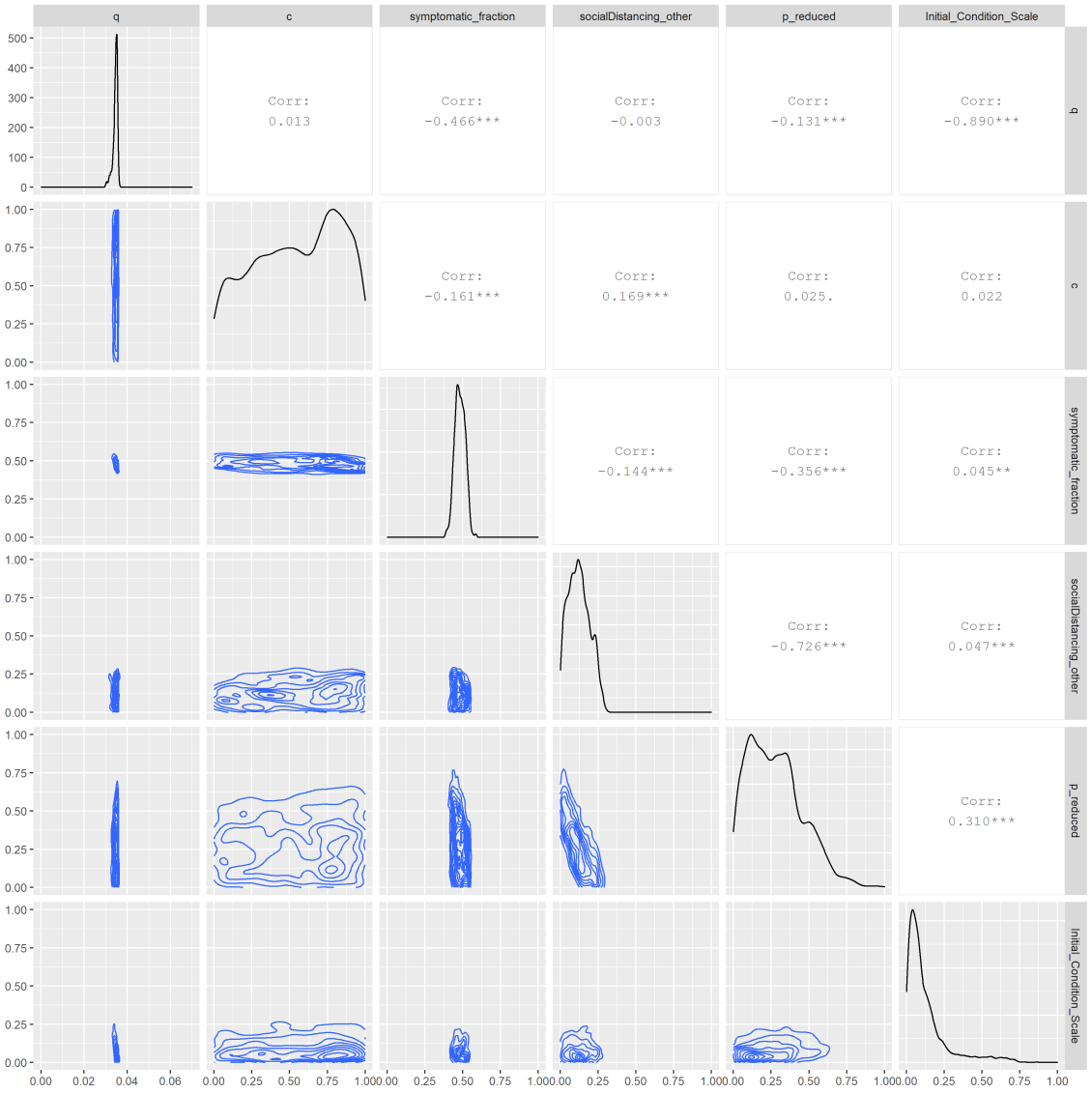

Figure S3: New York City Pairwise Parameter Correlations. Joint posterior distributions for pairs of parameters fitted to data from the New York City region for weekly reported deaths and seroprevalence estimates. Represented is the chain initialized with a minsearch algorithm.

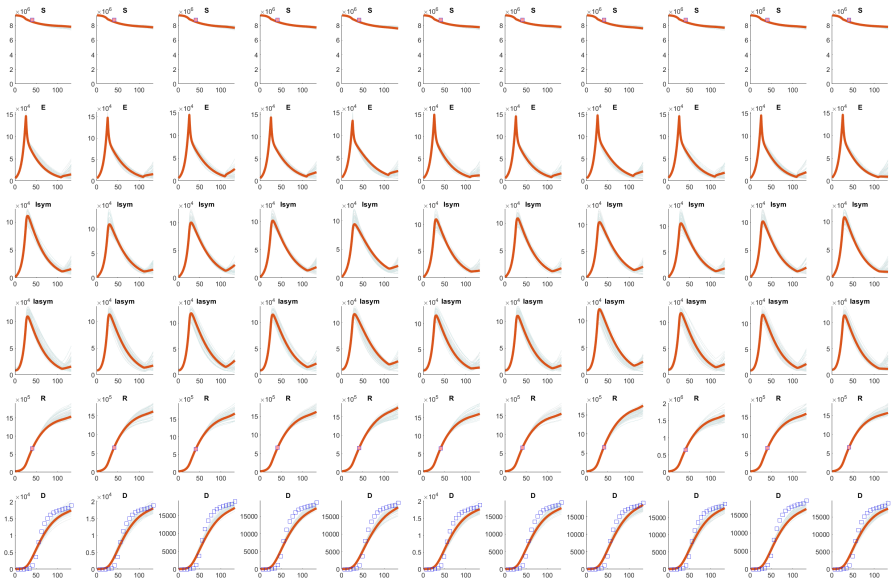

Figure S4: New York City Model Fits. We forward simulate a model using the maximum likelihood estimates of each parameter (red) and 100 random parameter set draws from the posterior distribution (gray). Cumulative deaths are plotted (blue squares), in addition to seroprevalence estimates (orange squares) in each location. Each column corresponds to an MCMC chain, with the first column corresponds to a chain which was initially seeded using a constrained 'minsearch' algorithm. Columns 2-11 correspond to MCMC chains 1-10, which are seeded randomly.

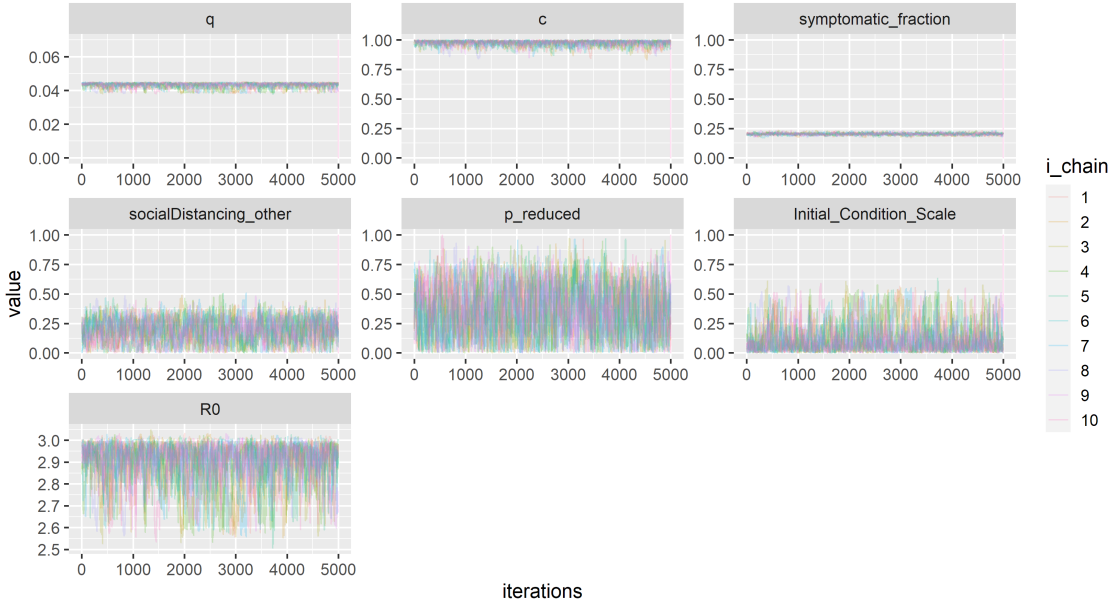

Figure S5: South Florida Post-burn-in MCMC Traceplots. Y-axis ranges are limited to show parameter search space constraints. R_0 traces are calculated from q and $symptomatic\_fraction$ traces.

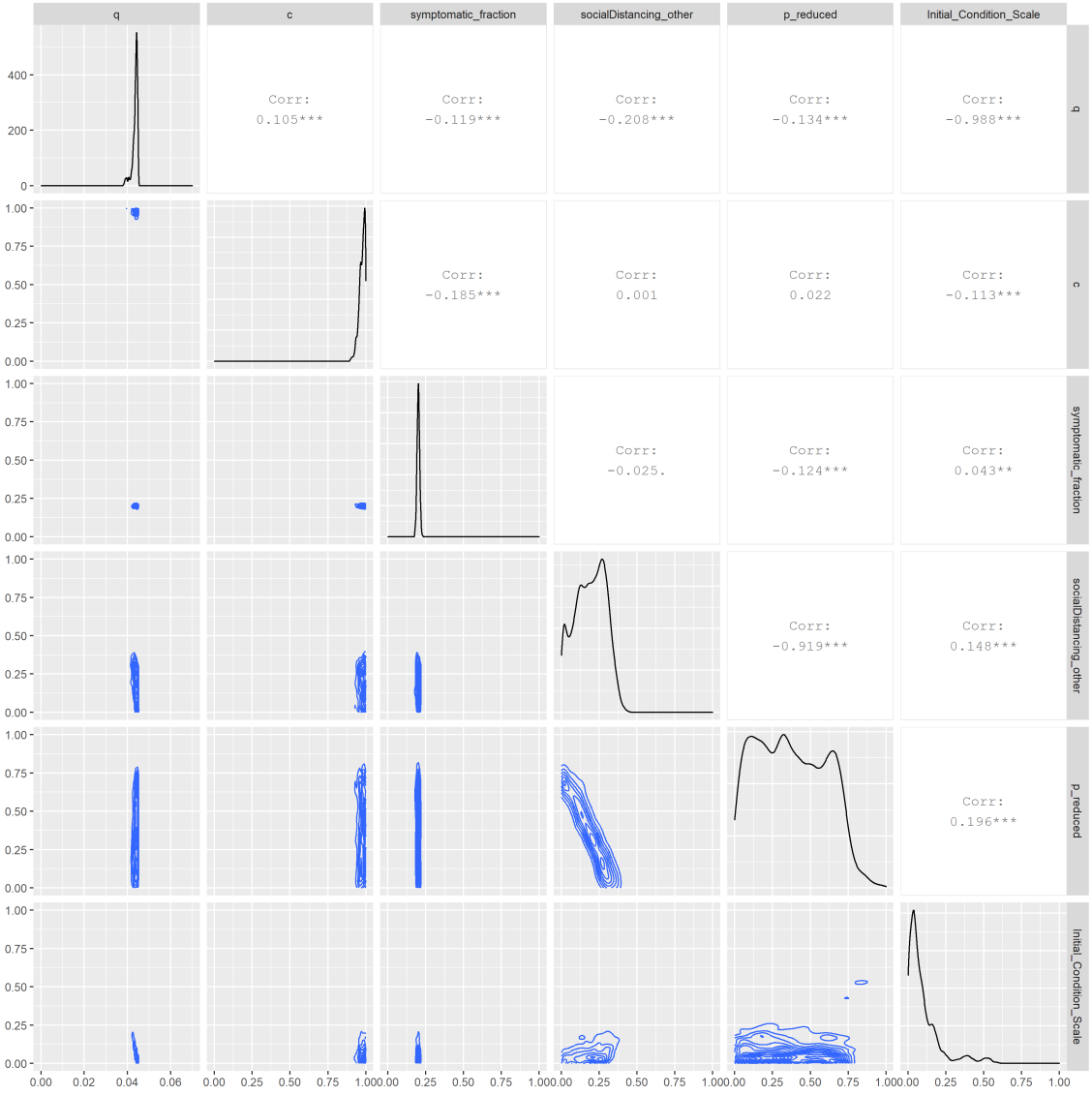

Figure S6: South Florida Pairwise Parameter Correlations. Joint posterior distributions for pairs of parameters fitted to data from the New York City region for weekly reported deaths and seroprevalence estimates.

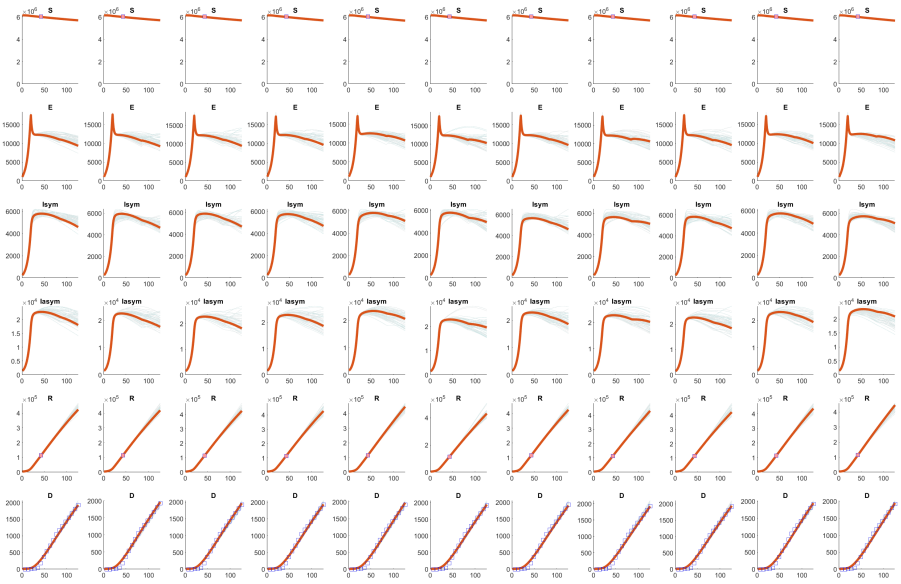

Figure S7: South Florida Model Fits. We forward simulate a model using the maximum likelihood estimates of each parameter (red) and 100 random parameter set draws from the posterior distribution (gray). Cumulative deaths are plotted (blue squares), in addition to seroprevalence estimates (orange squares) in each location. Each column corresponds to an MCMC chain, with the first column corresponds to a chain which was initially seeded using a constrained 'minsearch' algorithm. Columns 2-11 correspond to MCMC chains 1-10, which are seeded randomly.

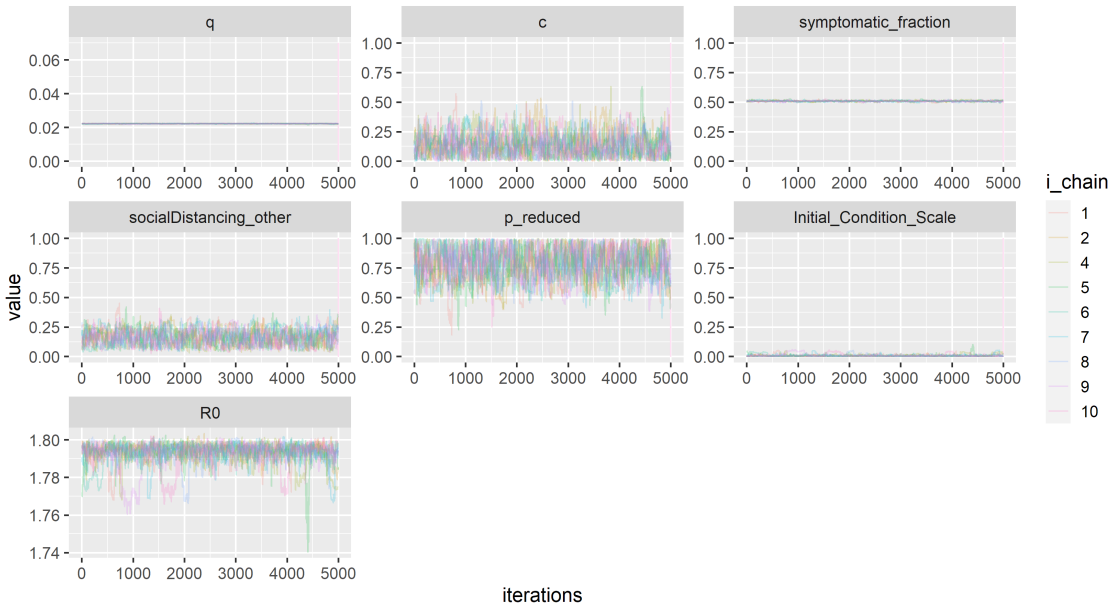

Figure S8: Washington Puget Sound Post-burn-in MCMC Traceplots. Y-axis ranges are limited to show parameter search space constraints. R_0 traces are calculated from q and $symptomatic\_fraction$ traces. Note that chain 3, which did not converge, was excluded from analyses.

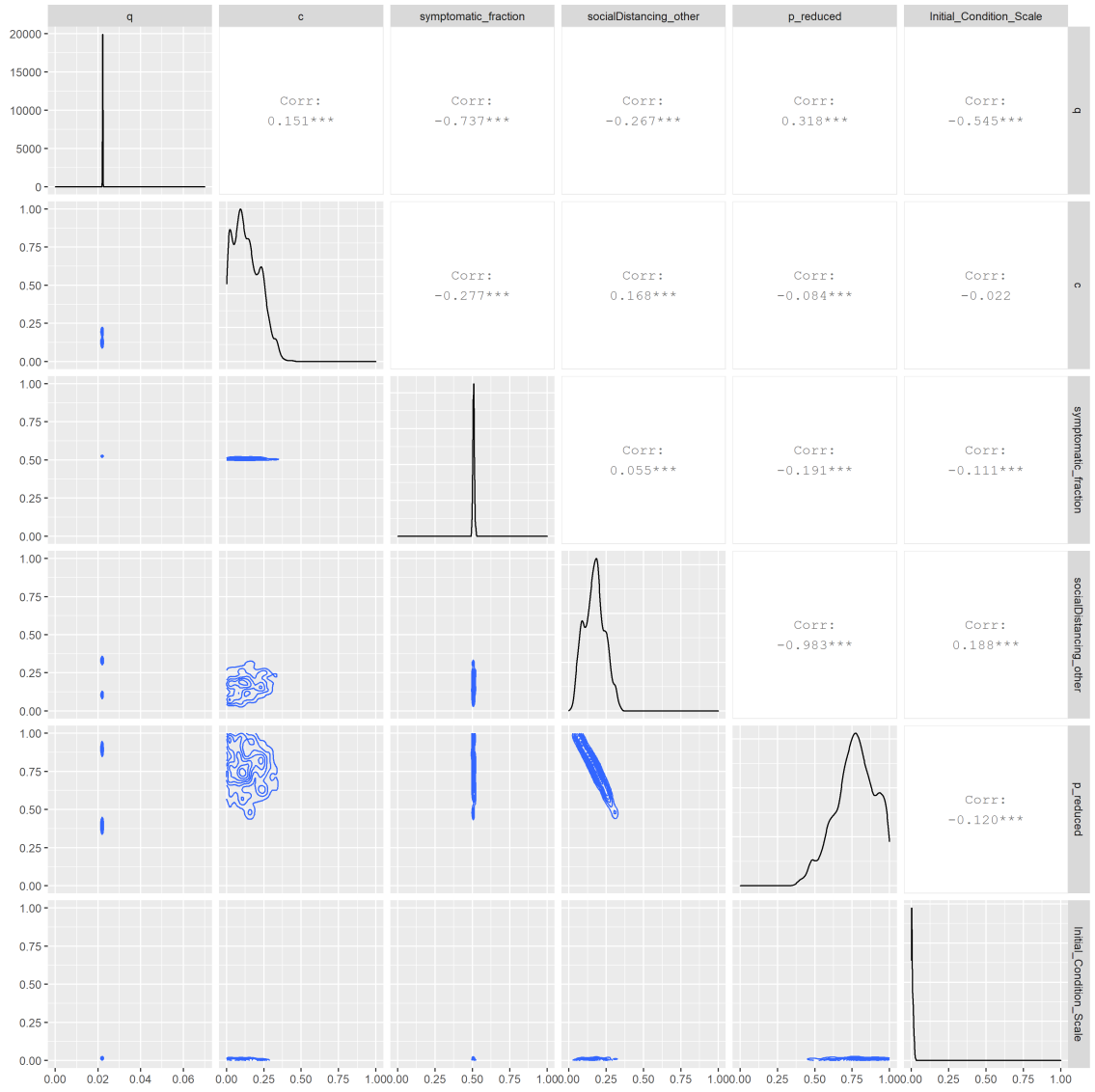

Figure S9: Washington Pairwise Parameter Correlations. Joint posterior distributions for pairs of parameters fitted to data from the New York City region for weekly reported deaths and seroprevalence estimates. Represented is the chain initialized with a minsearch algorithm.

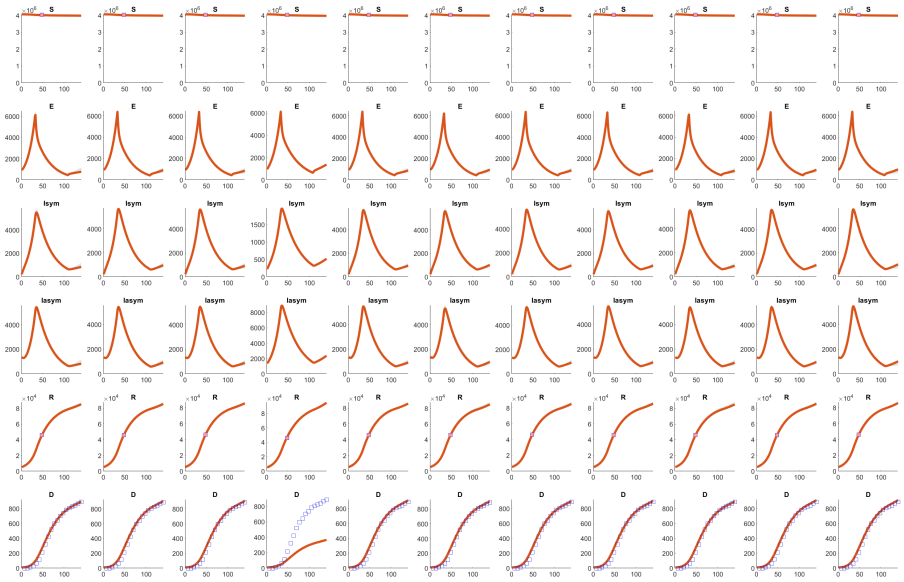

Figure S10: Washington Model Fits. We forward simulate a model using the maximum likelihood estimates of each parameter (red) and 100 random parameter set draws from the posterior distribution (gray). Cumulative deaths are plotted (blue squares), in addition to seroprevalence estimates (orange squares) in each location. Each column corresponds to an MCMC chain, with the first column corresponds to a chain which was initially seeded using a constrained 'minsearch' algorithm. Columns 2-11 correspond to MCMC chains 1-10, which are seeded randomly. Given that chain 3 (column 4) is a poor fit to the data and all other chains seemed to yield reasonable fits, we exclude chain 3 from further analyses.

Credible intervals width

The overall width of credible intervals (as shown in the main text) was determined by the value of c (Figure S11). As shown in the trace plots, the value of c was not identifiable from our model simulations, particularly for Washington and New York City, with a wide variety of initial values matching the initial dynamics. In South Florida, the fitted value of c was more constrained, yet model predictions still in large part depended on the ongoing level of social distancing. In part, this issue arose because the relaxation of social distancing in these two locations began after the first wave of the epidemic was largely complete (main text Figure 3), and thus there were few cases shortly after reopening with which to calibrate the dynamics. However, as the outbreak continued, this parameter was crucial for determining the number of deaths by the time shielding was implemented, and hence its ultimate impact. While adding to the length of the time series of deaths used to fit the model might have improved identifiability, ultimately the level of ongoing social distancing is likely to be highly time-varying. The width of the credible interval thus reflects the importance of ongoing social distancing to determine both the trajectory of the United States epidemic and the potential impact of any other control interventions.

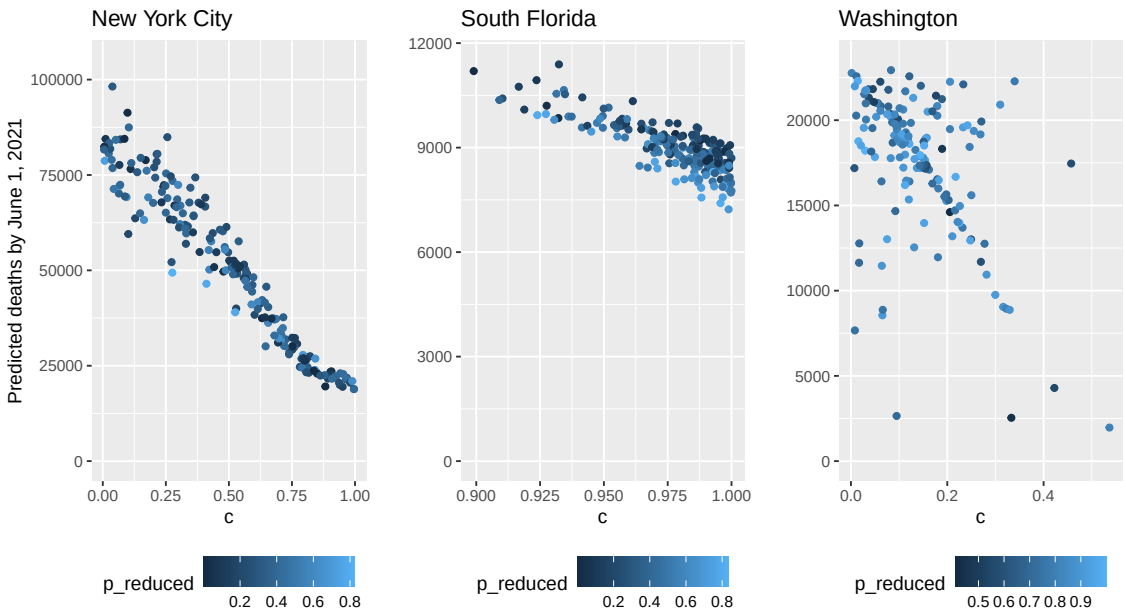

Figure S11: Number of deaths expected after 1 year (y-axis) for each setting (panels) without testing as a function of the degree of relaxation of social distancing (given by c, shown on the x-axis) and initial social distancing strength (colors indicate the value of $p_{reduced}$).

S4. R_0 Estimation

The dynamics of the system and R_0 are determined by how the outbreak would proceed at time zero in the absence of any interventions, and therefore depends on the fitted values of p and q, but not on any of the other fitted parameters. Therefore, we assume no testing at time 0, no social distancing, and no differences in worker contact levels (i.e., all groups mix at the population-average level prior to the outbreak). In this situation, there are only 3 population subgroups at time zero:

$$
\begin{aligned}
\frac{dE_{ch}}{dt} &= \lambda_{ch} S_{ch} - \gamma_e E_{ch} \\
\frac{dI_{s,ch}}{dt} &= \gamma_e E_{ch} p - \gamma_s I_{s,ch} \\
\frac{dI_{a,ch}}{dt} &= \gamma_e E_{ch}(1-p) - \gamma_a I_{a,ch} \\
\frac{dH_{s,ch}}{dt} &= \gamma_s I_{s,ch}(Hosp_{ch} - CritDie_{ch}) - \gamma_{hs} Hosp_{s,ch} \\
\frac{dH_{c,ch}}{dt} &= \gamma_s I_{s,ch} CritDie_{ch} - \gamma_{hc} Hosp_{c,ch} \\
\frac{dE_{ad}}{dt} &= \lambda_{ad} S_{ad} - \gamma_e E_{ad} \\
\frac{dI_{s,ad}}{dt} &= \gamma_e E_{ad} p - \gamma_s I_{s,ad} \\
\frac{dI_{a,ad}}{dt} &= \gamma_e E_{ad}(1-p) - \gamma_a I_{a,ad} \\
\frac{dH_{s,ad}}{dt} &= \gamma_s I_{s,ad}(Hosp_{ad} - CritDie_{ad}) - \gamma_{hs} Hosp_{s,ad} \\
\frac{dH_{c,ad}}{dt} &= \gamma_s I_{s,ad} CritDie_{ad} - \gamma_{hc} Hosp_{c,ad} \\
\frac{dE_{el}}{dt} &= \lambda_{el} S_{el} - \gamma_e E_{el} \\
\frac{dI_{s,el}}{dt} &= \gamma_e E_{el} p - \gamma_s I_{s,el} \\
\frac{dI_{a,el}}{dt} &= \gamma_e E_{el}(1-p) - \gamma_a I_{a,el} \\
\frac{dH_{s,el}}{dt} &= \gamma_s I_{s,el}(Hosp_{el} - CritDie_{el}) - \gamma_{hs} Hosp_{s,el} \\
\frac{dH_{c,el}}{dt} &= \gamma_s I_{s,el} CritDie_{el} - \gamma_{hc} Hosp_{c,el}
\end{aligned}
$$

The λ_i for each group is defined as follows.

$$
\lambda_{ch} = \frac{qx_{ch,ch}(asyI_{a,ch} + I_{s,ch})}{n_{ch}} + \frac{qx_{ch,ad}(asyI_{a,ad} + I_{s,ad})}{n_{ad}} + \frac{qx_{ch,el}(asyI_{a,el} + I_{s,el})}{n_{el}}
$$

$$
\lambda_{ad} = \frac{qx_{ad,ch}(asyI_{a,ch} + I_{s,ch})}{n_{ch}} + \frac{qx_{ad,ad}(asyI_{a,ad} + I_{s,ad})}{n_{ad}} + \frac{qx_{ad,el}(asyI_{a,el} + I_{s,el})}{n_{el}}
$$

$$\lambda_{el} = \frac{qx_{el,ch}(asyI_{a,ch} + I_{s,ch})}{n_{ch}} + \frac{qx_{el,ad}(asyI_{a,ad} + I_{s,ad})}{n_{ad}} + \frac{qx_{el,el}(asyI_{a,el} + I_{s,el})}{n_{el}}$$

The matrices $\mathcal{F}$ and $\mathcal{V}$ corresponding to these equations are:

$$\mathcal{F} = \begin{bmatrix}
0 & qx_{ch,ch} & qx_{ch,ch}{}^{asy} & 0 & 0 & 0 & qc_{ch,ad} & qx_{ch,ad}{}^{asy} & 0 & 0 & 0 & qx_{ch,el} & qx_{ch,el}{}^{asy} & 0 & 0 \\
0 & 0 & 0 & 0 & 0 & 0 & 0 & 0 & 0 & 0 & 0 & 0 & 0 & 0 & 0 \\
0 & 0 & 0 & 0 & 0 & 0 & 0 & 0 & 0 & 0 & 0 & 0 & 0 & 0 & 0 \\
0 & 0 & 0 & 0 & 0 & 0 & 0 & 0 & 0 & 0 & 0 & 0 & 0 & 0 & 0 \\
0 & 0 & 0 & 0 & 0 & 0 & 0 & 0 & 0 & 0 & 0 & 0 & 0 & 0 & 0 \\
0 & qx_{ad,ch} & qx_{ad,ch}{}^{asy} & 0 & 0 & 0 & qx_{ad,ad} & qx_{ad,ad}{}^{asy} & 0 & 0 & 0 & qx_{ad,el} & qx_{ad,el}{}^{asy} & 0 & 0 \\
0 & 0 & 0 & 0 & 0 & 0 & 0 & 0 & 0 & 0 & 0 & 0 & 0 & 0 & 0 \\
0 & 0 & 0 & 0 & 0 & 0 & 0 & 0 & 0 & 0 & 0 & 0 & 0 & 0 & 0 \\
0 & 0 & 0 & 0 & 0 & 0 & 0 & 0 & 0 & 0 & 0 & 0 & 0 & 0 & 0 \\
0 & 0 & 0 & 0 & 0 & 0 & 0 & 0 & 0 & 0 & 0 & 0 & 0 & 0 & 0 \\
0 & qx_{el,ch} & qx_{el,ch}{}^{asy} & 0 & 0 & 0 & qx_{el,ad} & qx_{el,ad}{}^{asy} & 0 & 0 & 0 & qx_{el,el} & qx_{el,el}{}^{asy} & 0 & 0 \\
0 & 0 & 0 & 0 & 0 & 0 & 0 & 0 & 0 & 0 & 0 & 0 & 0 & 0 & 0 \\
0 & 0 & 0 & 0 & 0 & 0 & 0 & 0 & 0 & 0 & 0 & 0 & 0 & 0 & 0 \\
0 & 0 & 0 & 0 & 0 & 0 & 0 & 0 & 0 & 0 & 0 & 0 & 0 & 0 & 0 \\
0 & 0 & 0 & 0 & 0 & 0 & 0 & 0 & 0 & 0 & 0 & 0 & 0 & 0 & 0
\end{bmatrix}$$

$$\mathcal{V} = \begin{bmatrix}
\gamma_e & 0 & 0 & 0 & 0 & 0 & 0 & 0 & 0 & 0 & 0 & 0 & 0 & 0 & 0 \\
-\gamma_e p & \gamma_s & 0 & 0 & 0 & 0 & 0 & 0 & 0 & 0 & 0 & 0 & 0 & 0 & 0 \\
-\gamma_e(1-p) & 0 & \gamma_a & 0 & 0 & 0 & 0 & 0 & 0 & 0 & 0 & 0 & 0 & 0 & 0 \\
0 & -\gamma_s(Hosp_{ch} - Crit_{ch}) & 0 & \gamma_{hs} & 0 & 0 & 0 & 0 & 0 & 0 & 0 & 0 & 0 & 0 & 0 \\
0 & -\gamma_s Crit_{ch} & 0 & 0 & \gamma_{hc} & 0 & 0 & 0 & 0 & 0 & 0 & 0 & 0 & 0 & 0 \\
0 & 0 & 0 & 0 & 0 & \gamma_e & 0 & 0 & 0 & 0 & 0 & 0 & 0 & 0 & 0 \\
0 & 0 & 0 & 0 & 0 & -\gamma_e p & \gamma_s & 0 & 0 & 0 & 0 & 0 & 0 & 0 & 0 \\
0 & 0 & 0 & 0 & 0 & -\gamma_e(1-p) & 0 & \gamma_a & 0 & 0 & 0 & 0 & 0 & 0 & 0 \\
0 & 0 & 0 & 0 & 0 & 0 & -\gamma_s(Hosp_{ad} - Crit_{ad}) & 0 & \gamma_{hs} & 0 & 0 & 0 & 0 & 0 & 0 \\
0 & 0 & 0 & 0 & 0 & 0 & -\gamma_s Crit_{ad} & 0 & 0 & \gamma_{hc} & 0 & 0 & 0 & 0 & 0 \\
0 & 0 & 0 & 0 & 0 & 0 & 0 & 0 & 0 & 0 & \gamma_e & 0 & 0 & 0 & 0 \\
0 & 0 & 0 & 0 & 0 & 0 & 0 & 0 & 0 & 0 & -\gamma_e p & \gamma_s & 0 & 0 & 0 \\
0 & 0 & 0 & 0 & 0 & 0 & 0 & 0 & 0 & 0 & -\gamma_e(1-p) & 0 & \gamma_a & 0 & 0 \\
0 & 0 & 0 & 0 & 0 & 0 & 0 & 0 & 0 & 0 & 0 & 0 & -\gamma_s(Hosp_{el} - Crit_{el} & \gamma_{hs} & 0 \\
0 & 0 & 0 & 0 & 0 & 0 & 0 & 0 & 0 & 0 & 0 & 0 & -\gamma_s CritDie_{el} & 0 & \gamma_{hc}
\end{bmatrix}$$

To derive an expression for R_0 we inverted the $\mathcal{V}$ matrix and multiplied by $\mathcal{F}$. The dominant eigenvalues of this matrix can be computed, but are very complex and are therefore not shown here. It is notable that because hospitalized cases do not contribute to the force of infection, the value of R_0 does not depend on γ_{hs} or γ_{hc}. We calculated the value of R_0 for each of the three locations based on the fitted values of p and q and the other relevant parameters.

S5. Contact matrices

Baseline contacts

Baseline contact matrices for 'work' contacts, 'school' contacts, 'home' contacts, and 'other' contacts were taken from [11]. To expand these baseline matrices to the 5 population groups in our model (separating the adult population into fc, rc, and h classes), we multiplied all contacts with adults $x_{i,ad}$ by the proportion of the adult population falling into each class. We define the fraction of the population falling in each working group as follows:

$$f.home = \frac{n_{home}}{n_{home} + n_{reduced} + n_{full}}$$
$$f.reduced = \frac{n_{reduced}}{n_{home} + n_{reduced} + n_{full}}$$
$$f.full = \frac{n_{full}}{n_{home} + n_{reduced} + n_{full}}$$

For baseline contact matrix values based on [11], we have:

$$x_{i,j} = \begin{bmatrix} x_{ch,ch} & x_{ch,ad} & x_{ch,el} \\ x_{ad,ch} & x_{ad,ad} & x_{ad,el} \\ x_{el,ch} & x_{el,ad} & x_{el,el} \end{bmatrix}$$

For simplicity, we assume that baseline interactions between worker subgroups are only assortative with respect to age (and not with respect to occupation type). To expand this matrix to a 5x5 matrix we use the following notation, where rows 2, 3, and 4 correspond to the work from home, reduced contact, and full contact occupation groups, respectively:

$$x_{i,j} = \begin{bmatrix} x_{ch,ch} & x_{ch,ad}f.home & x_{ch,ad}f.reduced & x_{ch,ad}f.full & x_{ch,el} \\ x_{ad,ch} & x_{ad,ad}f.home & x_{ad,ad}f.reduced & x_{ad,ad}f.full & x_{ch,el} \\ x_{ad,ch} & x_{ad,ad}f.home & x_{ad,ad}f.reduced & x_{ad,ad}f.full & x_{ch,el} \\ x_{ad,ch} & x_{ad,ad}f.home & x_{ad,ad}f.reduced & x_{ad,ad}f.full & x_{ch,el} \\ x_{el,ch} & x_{el,ad}f.home & x_{el,ad}f.reduced & x_{el,ad}f.full & x_{ch,el} \end{bmatrix}$$

Based on these proportions, we define $x_{i,h}$, $x_{i,rc}$, and $x_{i,fc}$ as follows:

$$x_{i,h} = x_{i,ad} f.home$$
$$x_{i,rc} = x_{i,ad} f.reduced$$
$$x_{i,fc} = x_{i,ad} f.full$$

Contacts under social distancing

After social distancing has begun, we assume that:

- Home contacts remain the same.
- Schools and daycares close.
- Only working age adults continue to work. Baseline workplace contacts for children and young adults under 20 years of age are nearly zero (average 0.84 contacts/day) and the average workplace contacts for the elderly is 0, so this does not appreciably impact our results.
- All working adults who are able work from home.
- Adults continuing to work outside the home reduce their workplace contacts by constant $p_{reduced}$.
- Other contacts are reduced by scalar constant sd_{other}.

The revised contact matrix for work contacts then becomes:

$$CM_{work} = \begin{bmatrix} 0 & 0 & 0 & 0 & 0 \\ 0 & 0 & 0 & 0 & 0 \\ x_{ad,ch}\mathrm{p}_{reduced} & x_{h,h}\mathrm{p}_{reduced} & x_{h,rc}\mathrm{p}_{reduced} & x_{h,fc}\mathrm{p}_{reduced} & x_{ch,el}\mathrm{p}_{reduced} \\ x_{fc,ch} & x_{fc,h} & x_{fc,rc} & x_{fc,fc} & x_{ch,el} \\ 0 & 0 & 0 & 0 & 0 \end{bmatrix}$$

The revised contact matrix for other contacts becomes:

$$CM_{other} = sd.other \times \begin{bmatrix} x_{ch,ch} & x_{ch,h} & x_{ch,rc} & x_{ch,fc} & x_{ch,el} \\ x_{h,ch} & x_{h,h} & x_{h,rc} & x_{h,fc} & x_{ch,el} \\ x_{rc,ch} & x_{rc,h} & x_{rc,rc} & x_{rc,f} & x_{ch,el} \\ x_{fc,ch} & x_{fc,h} & x_{fc,rc} & x_{fc,fc} & x_{ch,el} \\ x_{el,ch} & x_{el,h} & x_{el,rc} & x_{el,fc} & x_{ch,el} \end{bmatrix}$$

Contacts during initial relaxing of social distancing

When stay at home orders are initially lifted, we assume that:

- Home contacts remain the same.
- Adults who were working from home continue to work from home.

- Workers in reduced contact occupations increase their workplace contacts based on the intensity of social distancing maintained.
- Schools remain closed until September 1, 2020 in South Florida and until October 1, 2020 in New York City and Washington, after which time they reopen at 50% capacity.
- Other contacts continue to be reduced based on the intensity of social distancing maintained.

Contacts after testing begins

When testing begins, we assume that:

- Test-positive individuals move to the test positive group.
- Home contacts remain the same, but their distribution by test status is driven by the proportion of test-positives in the general population.
- Adults who were working from home may return to work if they test positive. Upon returning to work, their workplace contacts are assortative with respect to test status (but not with respect to occupation type).
- Workers in reduced contact occupations increase their workplace contacts based on the intensity of social distancing maintained. Work contacts are preferentially with test-positive individuals, as determined by α, or shielding strength.
- Other contacts are increased for test positive individuals to their pre-pandemic levels. Other contacts continue to be reduced for test negative/untested individuals based on the intensity of social distancing maintained. Other contacts are preferentially with test-positive individuals, as determined by α, or shielding strength.

After testing has begun, all contact matrices are dependent on the proportion of the population that has tested positive and been released from social distancing at time t. We define this proportion as $r_i(t)$, where $(1 - r_i(t))$ is the fraction of the population who has not yet tested positive.

We assume that social distancing parameters are relaxed from their initial values as follows:

$$p_{reduced} = 1 - (sd_{other} \times c)$$
$$p_{reduced} = 1 - (p_{reduced} \times c)$$

For contact matrices of work and 'other' contacts, we implement shielding factor α, which increases the probability of contacting a test-positive individual according to their prevalence in the population (achieved by multiplying expected contact rates due to prevalence by scaling factor $\alpha + 1$). To account for the fact that, when prevalence is high, $(\alpha + 1)r_i(t)$ may exceed 1, we introduce a variable $s_i(t)$:

$$s_i(t) = \begin{cases} (\alpha+1)r_i(t) & (\alpha+1)r_i(t) \leq 1 \\ 1 & (\alpha+1)r_i(t) \geq 1 \end{cases}$$

This shielding structure is similar to 'fixed shielding', previously described by Weitz et al [18] in that it preserves the baseline number of contacts and increases contacts for test positive individuals by $1 + \alpha$, as shown below:

$$x_0 = x_0 r_i(t) + x_0(1 - r_i(t))$$
$$x_0 = r_i(t)(\alpha + 1)x_0 + (x_0 - (\alpha + 1)r_i(t)x_0)$$

The structure of all three matrices (home, work, and other) is given by CM:

$$CM_{home} = \begin{bmatrix} r_{ch}(t)x_{ch,ch} & (1-r_{ch}(t))x_{ch,ch} & r_h(t)x_{ch,h} & (1-r_h(t))x_{ch,h} & r_{rc}(t)x_{ch,rc} & (1-r_{rc}(t))x_{ch,rc} & r_{fc}(t)x_{ch,fc} & (1-r_{fc}(t))x_{ch,fc} & r_{el}(t)x_{ch,el} & (1-r_{el}(t))x_{ch,el} \\ r_{ch}(t)x_{ch,ch} & (1-r_{ch}(t))x_{ch,ch} & r_h(t)x_{ch,h} & (1-r_h(t))x_{ch,h} & r_{rc}(t)x_{ch,rc} & (1-r_{rc}(t))x_{ch,rc} & r_{fc}(t)x_{ch,fc} & (1-r_{fc}(t))x_{ch,fc} & r_{el}(t)x_{ch,el} & (1-r_{el}(t))x_{ch,el} \\ r_{ch}(t)x_{h,ch} & (1-r_{ch}(t))x_{h,ch} & r_h(t)x_{h,h} & (1-r_h(t))x_{h,h} & r_{rc}(t)x_{h,rc} & (1-r_{rc}(t))x_{h,rc} & r_{fc}(t)x_{h,fc} & (1-r_{fc}(t))x_{h,fc} & r_{el}(t)x_{h,el} & (1-r_{el}(t))x_{h,el} \\ r_{ch}(t)x_{h,ch} & (1-r_{ch}(t))x_{h,ch} & r_h(t)x_{h,h} & (1-r_h(t))x_{h,h} & r_{rc}(t)x_{h,rc} & (1-r_{rc}(t))x_{h,rc} & r_{fc}(t)x_{h,fc} & (1-r_{fc}(t))x_{h,fc} & r_{el}(t)x_{h,el} & (1-r_{el}(t))x_{h,el} \\ r_{ch}(t)x_{rc,ch} & (1-r_{ch}(t))x_{rc,ch} & r_h(t)x_{rc,h} & (1-r_h(t))x_{rc,h} & r_{rc}(t)x_{rc,rc} & (1-r_{rc}(t))x_{rc,rc} & r_{fc}(t)x_{rc,fc} & (1-r_{fc}(t))x_{rc,fc} & r_{el}(t)x_{rc,el} & (1-r_{el}(t))x_{rc,el} \\ r_{ch}(t)x_{rc,ch} & (1-r_{ch}(t))x_{rc,ch} & r_h(t)x_{rc,h} & (1-r_h(t))x_{rc,h} & r_{rc}(t)x_{rc,rc} & (1-r_{rc}(t))x_{rc,rc} & r_{fc}(t)x_{rc,fc} & (1-r_{fc}(t))x_{rc,fc} & r_{el}(t)x_{rc,el} & (1-r_{el}(t))x_{rc,el} \end{bmatrix}$$

$$CM_{other} = \begin{bmatrix} 1 \\ sd.other2 \\ 1 \\ sd.other2 \\ 1 \\ sd.other2 \\ 1 \\ sd.other2 \end{bmatrix} \times \begin{bmatrix} s_{ch}(t)x_{ch,ch} & (1-s_{ch}(t))x_{ch,ch} & s_h(t)x_{ch,h} & (1-s_h(t))x_{ch,h} & s_{rc}(t)x_{ch,rc} & (1-s_{rc}(t))x_{ch,rc} & s_{fc}(t)x_{ch,fc} & (1-s_{fc}(t))x_{ch,fc} & s_{el}(t)x_{ch,el} & (1-s_{el}(t))x_{ch,el} \\ s_{ch}(t)x_{ch,ch} & (1-s_{ch}(t))x_{ch,ch} & s_h(t)x_{ch,h} & (1-s_h(t))x_{ch,h} & s_{rc}(t)x_{ch,rc} & (1-s_{rc}(t))x_{ch,rc} & s_{fc}(t)x_{ch,fc} & (1-s_{fc}(t))x_{ch,fc} & s_{el}(t)x_{ch,el} & (1-s_{el}(t))x_{ch,el} \\ s_{ch}(t)x_{h,ch} & (1-s_{ch}(t))x_{h,ch} & s_h(t)x_{h,h} & (1-s_h(t))x_{h,h} & s_{rc}(t)x_{h,rc} & (1-s_{rc}(t))x_{h,rc} & s_{fc}(t)x_{h,fc} & (1-s_{fc}(t))x_{h,fc} & s_{el}(t)x_{h,el} & (1-s_{el}(t))x_{h,el} \\ s_{ch}(t)x_{h,ch} & (1-s_{ch}(t))x_{h,ch} & s_h(t)x_{h,h} & (1-s_h(t))x_{h,h} & s_{rc}(t)x_{h,rc} & (1-s_{rc}(t))x_{h,rc} & s_{fc}(t)x_{h,fc} & (1-s_{fc}(t))x_{h,fc} & s_{el}(t)x_{h,el} & (1-s_{el}(t))x_{h,el} \\ s_{ch}(t)x_{rc,ch} & (1-s_{ch}(t))x_{rc,ch} & s_h(t)x_{rc,h} & (1-s_h(t))x_{rc,h} & s_{rc}(t)x_{rc,rc} & (1-s_{rc}(t))x_{rc,rc} & s_{fc}(t)x_{rc,fc} & (1-s_{fc}(t))x_{rc,fc} & s_{el}(t)x_{rc,el} & (1-s_{el}(t))x_{rc,el} \\ s_{ch}(t)x_{rc,ch} & (1-s_{ch}(t))x_{rc,ch} & s_h(t)x_{rc,h} & (1-s_h(t))x_{rc,h} & s_{rc}(t)x_{rc,rc} & (1-s_{rc}(t))x_{rc,rc} & s_{fc}(t)x_{rc,fc} & (1-s_{fc}(t))x_{rc,fc} & s_{el}(t)x_{rc,el} & (1-s_{el}(t))x_{rc,el} \\ s_{ch}(t)x_{fc,ch} & (1-s_{ch}(t))x_{fc,ch} & s_h(t)x_{fc,h} & (1-s_h(t))x_{fc,h} & s_{rc}(t)x_{fc,rc} & (1-s_{rc}(t))x_{fc,rc} & s_{fc}(t)x_{fc,fc} & (1-s_{fc}(t))x_{fc,fc} & s_{el}(t)x_{fc,el} & (1-s_{el}(t))x_{fc,el} \\ s_{ch}(t)x_{fc,ch} & (1-s_{ch}(t))x_{fc,ch} & s_h(t)x_{fc,h} & (1-s_h(t))x_{fc,h} & s_{rc}(t)x_{fc,rc} & (1-s_{rc}(t))x_{fc,rc} & s_{fc}(t)x_{fc,fc} & (1-s_{fc}(t))x_{fc,fc} & s_{el}(t)x_{fc,el} & (1-s_{el}(t))x_{fc,el} \\ s_{ch}(t)x_{el,ch} & (1-s_{ch}(t))x_{el,ch} & s_h(t)x_{el,h} & (1-s_h(t))x_{el,h} & s_{rc}(t)x_{el,rc} & (1-s_{rc}(t))x_{el,rc} & s_{fc}(t)x_{el,fc} & (1-s_{fc}(t))x_{el,fc} & s_{el}(t)x_{el,el} & (1-s_{el}(t))x_{el,el} \\ s_{ch}(t)x_{el,ch} & (1-s_{ch}(t))x_{el,ch} & s_h(t)x_{el,h} & (1-s_h(t))x_{el,h} & s_{rc}(t)x_{el,rc} & (1-s_{rc}(t))x_{el,rc} & s_{fc}(t)x_{el,fc} & (1-s_{fc}(t))x_{el,fc} & s_{el}(t)x_{el,el} & (1-s_{el}(t))x_{el,el} \end{bmatrix}$$

$$CM_{work} = \begin{bmatrix} 0 \\ 0 \\ 1 \\ 0 \\ produced2 \\ produced2 \\ 1 \\ 1 \\ 0 \\ 0 \end{bmatrix} \times \begin{bmatrix} 0 & 0 & 0 & 0 & 0 & 0 & 0 & 0 & 0 & 0 \\ 0 & 0 & 0 & 0 & 0 & 0 & 0 & 0 & 0 & 0 \\ x_{h,ch} & 0 & x_{h,h} & 0 & x_{h,rc} & 0 & x_{h,fc} & 0 & x_{h,el} & 0 \\ 0 & 0 & 0 & 0 & 0 & 0 & 0 & 0 & 0 & 0 \\ s_{ch}(t)x_{rc,ch} & (1-s_{ch}(t))x_{rc,ch} & s_h(t)x_{rc,h} & (1-s_h(t))x_{rc,h} & s_{rc}(t)x_{rc,rc} & (1-s_{rc}(t))x_{rc,rc} & s_{fc}(t)x_{rc,fc} & (1-s_{fc}(t))x_{rc,fc} & s_{el}(t)x_{rc,el} & (1-s_{el}(t))x_{rc,el} \\ s_{ch}(t)x_{rc,ch} & (1-s_{ch}(t))x_{rc,ch} & s_h(t)x_{rc,h} & (1-s_h(t))x_{rc,h} & s_{rc}(t)x_{rc,rc} & (1-s_{rc}(t))x_{rc,rc} & s_{fc}(t)x_{rc,fc} & (1-s_{fc}(t))x_{rc,fc} & s_{el}(t)x_{rc,el} & (1-s_{el}(t))x_{rc,el} \\ 0 & 0 & 0 & 0 & 0 & 0 & 0 & 0 & 0 & 0 \\ 0 & 0 & 0 & 0 & 0 & 0 & 0 & 0 & 0 & 0 \end{bmatrix}$$

S6. Overall contact reductions by location

Location	Reduction in work contacts for adults	Reduction in other contacts for all groups	Reduction in total contacts		
			Children	Adults	Elderly
New York City	52.3%	43.9%	33.8%	37.6%	25.5%
South Florida	70.2%	78.4%	45.8%	56.1%	44.8%
Washington	32.1%	10.5%	21.9%	18.6%	6.9%

Table S3: Steady state reduction in contacts by location after stay-at-home orders are lifted and schools reopen

References

[1] Havers FP, Reed C, Lim T, Montgomery JM, Klena JD, Hall AJ, et al. Seroprevalence of Antibodies to SARS-CoV-2 in 10 Sites in the United States, March 23-May 12, 2020. JAMA Internal Medicine. 2020 Jul;.

[2] He X, Lau EHY, Wu P, Deng X, Wang J, Hao X, et al. Temporal dynamics in viral shedding and transmissibility of COVID-19. Nature Medicine. 2020 Apr;p. 1–4. Publisher: Nature Publishing Group. Available from: https://www.nature.com/articles/s41591-020-0869-5.

[3] Kissler SM, Tedijanto C, Goldstein E, Grad YH, Lipsitch M. Projecting the transmission dynamics of SARS-CoV-2 through the postpandemic period. Science. 2020 Apr;p. eabb5793. Available from: https://www.sciencemag.org/lookup/doi/10.1126/science.abb5793.

[4] Rees EM, Nightingale ES, Jafari Y, Waterlow N, Clifford S, Pearson CAB, et al. COVID-19 length of hospital stay: a systematic review and data synthesis. BMC Medicine. 2020;(270).

[5] Ferguson N. Report 9: Impact of non-pharmaceutical interventions (NPIs) to reduce COVID-19 mortality and healthcare demand;. Available from: https://www.imperial.ac.uk/media/imperial-college/medicine/sph/ide/gida-fellowships/Imperial-College-COVID19-NPI-modelling-16-03-2020.pdf.

[6] Li R, Pei S, Chen B, Song Y, Zhang T, Yang W, et al. Substantial undocumented infection facilitates the rapid dissemination of novel coronavirus (SARS-CoV2). Science. 2020 Mar;p. eabb3221. Available from: https://www.sciencemag.org/lookup/doi/10.1126/science.abb3221.

[7] CDCMMWR. Severe Outcomes Among Patients with Coronavirus Disease 2019 (COVID-19) in United States, February 12–March 16, 2020. MMWR Morbidity and Mortality Weekly Report. 2020;69. Available from: https://www.cdc.gov/mmwr/volumes/69/wr/mm6912e2.htm.

[8] Zhou F, Yu T, Du R, Fan G, Liu Y, Liu Z, et al. Clinical course and risk factors for mortality of adult inpatients with COVID-19 in Wuhan, China: a retrospective cohort study. The Lancet. 2020 Mar;395(10229):1054–1062. Publisher: Elsevier. Available from: https://www.thelancet.com/journals/lancet/article/PIIS0140-6736(20)30566-3/abstract.

[9] Health CfDaR. EUA Authorized Serology Test Performance. FDA. 2020 May;Publisher: FDA. Available from: https://www.fda.gov/medical-devices/emergency-situations-medical-devices/eua-authorized-serology-test-performance.

[10] Bureau UC. Age and Sex Composition in the United States by County: 2015;. Available from: https://www2.census.gov/programs-surveys/popest/datasets/2010-2019/counties/.

[11] Prem K, Cook AR, Jit M. Projecting social contact matrices in 152 countries using contact surveys and demographic data. PLOS Computational Biology. 2017 Sep;13(9):e1005697. Publisher: Public Library of Science. Available from: https://journals.plos.org/ploscompbiol/article?id=10.1371/journal.pcbi.1005697.

[12] May 2019 OES National Industry-Specific Occupational Employment and Wage Estimates;. Library Catalog: www.bls.gov. Available from: https://www.bls.gov/oes/current/oessrci.htm.

[13] Bureau UC. Age and Sex Composition in the United States: 2018;. Available from: https://www.census.gov/data/tables/2018/demo/age-and-sex/2018-age-sex-composition.html.

[14] Times NY. See how all 50 states are reopening (and closing again);. Available from: https://www.nytimes.com/interactive/2020/us/states-reopen-map-coronavirus.html.

[15] local C. Visualizing the impact of policies on COVID-19 response; 2020. Available from: https://www.covid-local.org/amp/.

[16] Government MDC. Stand up Miami;. Available from: https://www.miamigov.com/Government/Stand-Up-Miami.

[17] Lambert B. A Student's Guide to Bayesian Statistics. SAGE; 2018.

[18] Weitz JS, Beckett SJ, Coenen AR, Demory D, Dominguez-Mirazo M, Dushoff J, et al. Modeling shield immunity to reduce COVID-19 epidemic spread. Nature Medicine. 2020;26:849–854. Available from: http://www.nature.com/articles/s41591-020-0895-3.